

# The Surface Accelerations Reference — A Large-scale, Interactive Catalog of Passenger Vehicle Accelerations

Gibran Ali, Shane McLaughlin and Mehdi Ahmadian

Abstract—There is a need for a large-scale, real world, diverse, and context rich vehicle acceleration catalog that can be used to design, analyze, and compare various intelligent transportation systems. This paper fulfills three primary objectives. First, it provides such a catalog through the Surface Accelerations Reference, which is openly available as an interactive analytics tool as well as an open and downloadable dataset. The Surface Accelerations Reference statistically describes the driving profiles of about 3,500 individuals contributing 34 million miles of continuous driving data collected in the Second Strategic Highway Research Program Naturalistic Driving Study (SHRP 2 NDS). These profiles were created by summarizing billions of longitudinal and lateral acceleration epochs experienced by the participants. Second, this paper introduces a standardized methodology for creating such a catalog so that similar acceleration profiles can be produced for other human cohorts or automated driving systems. Finally, the data are used to analyze the effect of roadway speed category on the rates of lateral and longitudinal acceleration epochs at various thresholds. It is observed that, for the median driver, the rates of epochs are upto 3 orders of magnitude higher on low-speed roads as compared to high-speed roads. This catalog will facilitate intelligent vehicle system designers to compare and tune their systems for safer driving experiences. It will also allow agencies with similar data to create comparable catalogs facilitating safety and behavioral comparisons between populations.

Index Terms—vehicle accelerations, driving style, driving comfort, big data analytics, autonomous vehicle driving style

## Nomenclature

$\lambda_z$	The rate of epochs corresponding to the $Z^{th}$ percentile value
$D_T$	Total distance traveled by a participant
$N_T$	Total number of epochs experienced by a driver
$N_X$	Number of epochs stronger than $X(g)$ experienced by a driver
$R_X$	Rate of epochs stronger than $X(g)$ per mile

G. Ali is with the Division of Data and Analytics, Virginia Tech Transportation Institute (email: gali@vtti.vt.edu)  
 S. McLaughlin is with Great Iris LLC (email: shane.mclaughlin@greatiris.com)  
 M. Ahmadian is with department of Mechanical Engineering, Virginia Tech (email: ahmadian@vt.edu)

CAN Controller Area Network

DAS Data Acquisition System

GPS Global Positioning System

SHRP 2 NDS The Second Strategic Highway Research Program Naturalistic Driving Study

## I. Introduction

The purpose of this project was to catalog longitudinal and lateral accelerations experienced in passenger vehicles and create an easily accessible dataset for users from a variety of fields. The Second Strategic Highway Research Program Naturalistic Driving Study (SHRP 2 NDS), the largest collection of naturalistic driving data to date, is an ideal data set to create such a catalog, with more than 34 million miles of data collected from a diverse set of participants [1]. The SHRP 2 NDS dataset was analyzed to create the Surface Accelerations Reference, which describes the acceleration norms and distributions of the 3,500 participants in the study.

This catalog of accelerations experienced in passenger vehicles will be valuable for users in a number of fields [2]–[4]. For example, considerable work has been done to model behavior, determine driving style and detect anomalous driving events using vehicle accelerations and other driving parameters [martinez\_driving\_2018, 5]–[17]. However, such research has mostly relied on small studies, nonrepresentative experiments, or test track data. The surface accelerations reference provides a dataset that is sufficient to describe thousands of individuals, support exploration of numerous groupings of individual styles, and quantify the effect of a broad range of roadway environments, traffic conditions, and vehicle classes.

Advanced driver assistance systems and automated driving systems will need to operate within the expectations of passengers as well as surrounding road users. Automated systems that assist drivers or fully autonomous vehicles will likely benefit from control that feels comfortable and natural [18]. These systems also rely on predicting the behavior of other road users to keep occupants safe. Both developers and policy

makers will benefit from objective understanding of the probability of acceleration behavior in a given context and the driving behavior of different road users.

In addition, roadway engineers consider vehicle kinematic parameters, such as longitudinal and lateral accelerations, speed, etc. to design roadways [19]. Often, such parameters come from models that were developed decades ago, in constrained experimental conditions, and which do not reflect current vehicle specifications [20]. Sometimes, such models are purely based on vehicle characteristics and do not reflect driver preferences or usage patterns [21]. The Surface Acceleration Reference, which represents the driving patterns of a diverse driver demographics and vehicle classes in a broad range of conditions, will therefore also be beneficial to roadway planners and departments of transportation.

Driver behavior research, which has traditionally relied on using adverse driving events to identify and evaluate risky driving behavior [22]–[24], can also benefit from establishing kinematics-based surrogate measures to classify risky driving [17], [25], [26]. Doing so would allow the prevention of safety critical events by identifying at-risk drivers and providing adequate driver training [27], [28]. Driver behavior researchers are also interested in categorizing various driving styles, such as sporty, aggressive, conservative, etc., and determining their relationship with risky driving. The Surface Acceleration Reference, based on SHRP 2 data, which also includes driver crash involvement, would greatly benefit such researchers, as a driver’s kinematic profile could be easily linked to their crash rates.

Many insurance companies have started pay-as-you-drive programs that incentivize good driving through better insurance rates [29]–[32]. The Surface Acceleration Reference will also be useful to companies behind such programs, as it would let them compare the kinematic profiles of their customers with a dataset that includes data from a broader sensor suite as well as a range of demographic measures and risk analyses. This catalog also has the potential to serve as a standard within the industry, making the process transparent and comprehensible for customers. Practitioners from other fields, such as traffic modeling, crash reconstruction, ISO standard development, etc., can also greatly benefit from this comprehensive acceleration catalog [33]–[35].

A number of studies have been conducted on understanding the acceleration preferences of drivers and passengers [36]–[41]. These studies provide valuable insights but have not been adopted as a cross-discipline reference on accelerations for various reasons, such as subjective interpretation of surveys; datasets being small, non-representative, or outdated; or lack of standard methods. These shortcomings had to be taken into consideration when developing the Surface Acceleration

Reference.

To create a comprehensive acceleration catalog that can serve as an industry standard across various research fields, five major challenges need to be overcome. These challenges can be characterized into data scale, algorithm standardization, data correction, result interpretability, and output accessibility. The Surface Accelerations Reference addresses all these challenges and therefore is an ideal candidate to be used as a standard of comparison across various fields.

First, the underlying dataset needed to generate such a catalog must be diverse, large, and contain high quality data. The SHRP 2 dataset was designed to be such a dataset. More than 3,500 participants were chosen from six locations across the country and were representative of all ages, genders, ethnicities, races, levels of education, and socioeconomic statuses [1]. Though there are differences between the SHRP 2 sample population and U.S. national statistics, SHRP 2 data are fairly representative of the nation’s population [42]. The SHRP 2 dataset is also the largest collection of naturalistic driving data, with more than 34 million miles of recorded data, including recordings from four video feeds (front, rear, and two in cabin views); various vehicle network variables such as speed, gas pedal input, brake state, etc.; location data in the form of GPS coordinates; and kinematic measures from an inertial measurement unit (IMU). A major advantage of such a dataset is that video feeds often provide additional context that helps validate outliers and detect malfunctioning sensors. The SHRP 2 dataset also has the advantage of containing recordings of more natural behaviors than datasets from studies where participants self-reported, drove with a researcher, or were enrolled for a shorter period of time. The lack of a standard acceleration catalog to date was in part due to the lack of a dataset that fulfilled all the requirements.

Second, for an acceleration catalog to be used across disciplines, there is a need for standardization of event definitions as well as the definition of rates. As various fields use different measures to compare event rarity, it is important to develop standard measures that can be used against other existing measures. For this purpose, an epoch definition, explained in the methodology section, was created and documented for a standardized acceleration epoch.

Third, collection over a long period of time is necessary to answer questions of interest related to accelerations, but IMU data are prone to noise and sources of error such as bias and drift. The process used to generate an acceleration catalog should recognize such errors and incorporate processes to isolate problematic data. On a related note, the scale of data processing requires considerable computing resources as well as efficient

algorithms.

Fourth, the output of such a catalog should be usable by practitioners from various fields. This poses multiple challenges as various disciplines are inclined to using different tools and rating scales in their analyses. To further ensure the Surface Acceleration Reference’s broad utility, the acceleration epoch identification, summarization algorithms, and methods for aggregating accelerations and generating participant driving profiles are well documented in this paper to ensure reproducibility. Finally, a consolidated acceleration profile table is available to practitioners from various fields through a downloadable CSV file as well as an interactive visualization. The interactive visualization can be accessed through any web browser and allows users to compare various participant groups based on age, location, gender, and vehicle class.

## II. Methodology

The Surface Accelerations Reference consists of an acceleration profile for each driver (or driver-vehicle combination if a participant drove more than one vehicle) created by analyzing their entire driving history in the SHRP 2 dataset. Figure 1 shows the data flow for creation of the Surface Accelerations Reference.

The acceleration data was collected from the participants’ vehicles from 2010 to 2013, using a triaxial accelerometer (LIS3LV02DQ1) and in-house data acquisition system (DAS)[43]. The data is sampled at 500 Hz but decimated down to 10 Hz in post-processing on the DAS itself. The decimated data, which is used for the analysis presented in this study, consists of the average of consecutive 50-point windows. Each average represents one data point for the decimated data. The averaging process behaves much like a low-pass filter, in which the high-frequency dynamics are de-emphasized in favor of the low-frequency or general trends in the data.

The original sensor-based time series data was read from the db2 database and analyzed by an algorithm that identified acceleration epochs. Each acceleration epoch was summarized as a multi feature data point and written to a database table. After the acceleration analysis algorithm was run on the entire SHRP 2 dataset, a profile generation algorithm aggregated all summarized accelerations in a participant’s history and created an acceleration profile. The acceleration profile contains about 400 data points for each of the 3,670 driver-vehicle combinations and can be stored in either a database or a downloadable CSV file. These acceleration profiles are made available as a downloadable CSV file as well as an interactive visualization through a web interface that lets users from a wide variety of fields parse data to answer questions relevant to their area of interest.

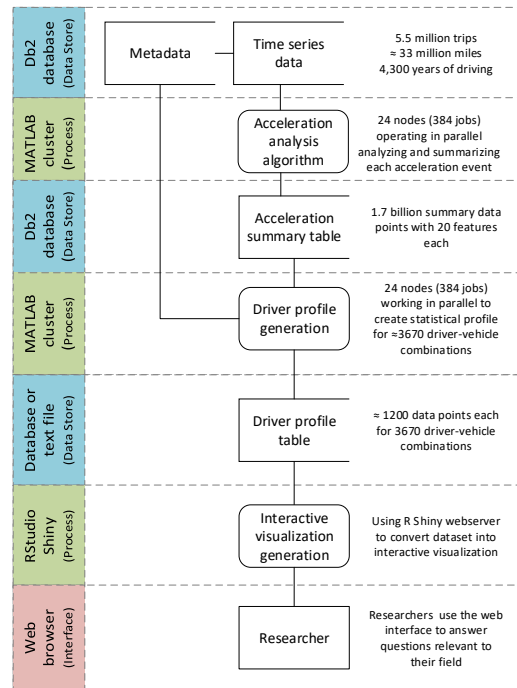


Figure 1: Data flow for creation of the Surface Accelerations Reference.

The creation of the Surface Acceleration Reference consisted of different processes that can be categorized into three stages: (1) identifying and summarizing acceleration epochs from time series data, (2) creating acceleration profiles from summarized epochs, and (3) generating an interactive visualization comparing these acceleration profiles.

### A. Identifying and Summarizing Acceleration Epochs

An algorithm was developed to read time series data from the database, identify epochs of longitudinal and lateral acceleration, summarize them, and write the summary to a table. The algorithm analyzed 10 variables, described in Table I, for every trip in the SHRP 2 dataset. The summarized epochs were linked to the original file and its associated metadata using a unique identifier and timestamps. Metadata associated with each trip included in the Surface Accelerations Reference is listed in Table II.

To efficiently process the vast amount of data, a Db2 database cluster and a computing cluster were used to run 384 instances of the algorithm in parallel. The algorithm first ingested all the variables from the Db2 database cluster. The signals were then cleaned and pre-processed by removing invalid values, deleting repeating timestamps, and clearing artifacts. As Table I shows, the original variables had different sampling rates. To make the algorithm more efficient, all variables were

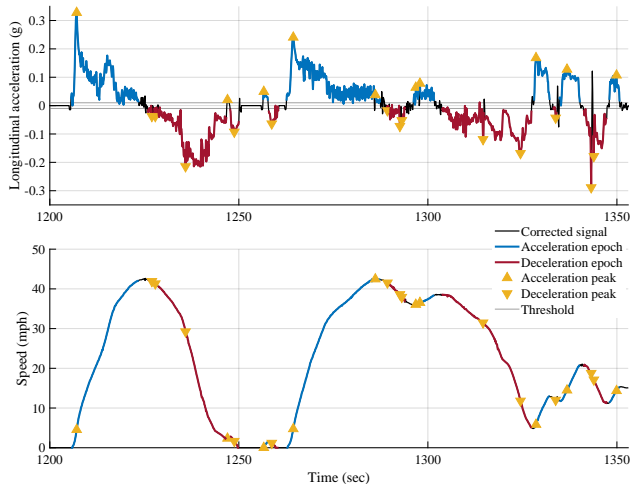


Figure 2: Identifying acceleration and deceleration epochs in longitudinal acceleration and speed time series data.

interpolated to align on a common timestamp series. After the variables were standardized as described above, longitudinal acceleration, lateral acceleration, and yaw rate were analyzed to find epochs. Having a standardized method to identify epochs that could be replicated on other studies was vital to the success of this project. An acceleration event or epoch is the duration for which the absolute value of a signal is continuously greater than a threshold value. For longitudinal and lateral accelerations, this value is  $\pm 0.01(g)$  and for yaw rate the threshold value is  $\pm 1 \text{ deg/sec}$ . The threshold values were chosen to ensure that fluctuations around the noise floor were not considered events, while still including cases that were quite low in amplitude [44]. Figure 2 shows the longitudinal acceleration and speed signals and illustrate the selection of acceleration and deceleration epochs and their peaks.

One of the challenges of analyzing acceleration signals is that when a vehicle is stopped on a slope, the accelerometer output shows a constant non zero value. According to the epoch definition, this would constitute an acceleration or deceleration epoch. To avoid these false positives, a method was developed where the acceleration signal was made equal to zero if the speed of the vehicle was zero and if the moving standard deviation of the acceleration signal was below 0.01. This ensured that these potential false positives would not be identified as epochs and at the same time that the start and end of the acceleration epochs would be set appropriately given the speed signal lag relative to the acceleration signal. A comparison between the original and the modified acceleration signals is shown in Figure 4. The effect of road grade on the absolute value of acceleration was not taken into account as it was assumed the the vehicle would be going up and down grades an equal number of

times, causing the change in absolute acceleration values to cancel each other out.

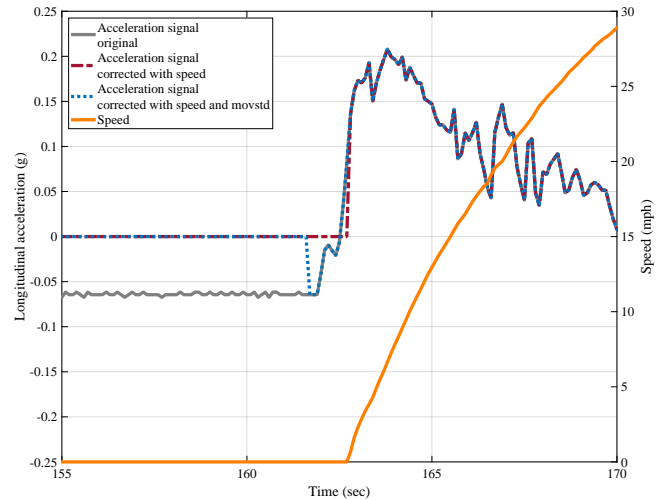


Figure 3: Comparing acceleration signal correction using speed and moving standard deviation.

A similar approach was used to identify epochs of lateral acceleration and yaw rate. Once the epochs were identified, the algorithm summarized each acceleration epoch and generated statistical measures described in Table III. These measures fall into three categories,

- 1) Trip properties, such as unique trip ID and timestamp within trip. These variables are useful to link each epoch to other metadata, such as driver, vehicle, road type on which the epoch happened, etc., associated with the trip.
- 2) Epoch properties, such as maximum value of signal in epoch, average value, distance traveled, etc. These summary variables provide additional details about the data as well as a means of qualifying epochs.
- 3) Variables describing driver inputs, such as the duration of brake pedal being pressed. These are useful for filtering and qualifying epochs based on driver inputs.
- 4) Variables describing roadway characteristics, such as road functional class and speed category [45]–[47]. These are valuable for contextualizing each event based on the road type.

Similar tables were created for lateral acceleration and yaw rates. A total of 1.7 billion summarized points were created and stored in a relational database. The table structure not only facilitates the creation of driver acceleration profiles but can also be used for contextualizing driving data in the SHRP 2 database using machine learning algorithms.

Table I: A description of the variables used to create the Surface Accelerations Reference.

Variable	Variable description	Source	Frequency
accel_x	Longitudinal acceleration	DAS IMU	10 Hz
accel_y	Lateral acceleration	DAS IMU	10 Hz
accel_z	Vertical acceleration	DAS IMU	10 Hz
gyro_x	Roll rate	DAS IMU	10 Hz
gyro_y	Pitch rate	DAS IMU	10 Hz
gyro_z	Yaw rate	DAS IMU	10 Hz
speed_network	Vehicle speed	Vehicle CAN	Variable (1-100 Hz)
speed_gps	Vehicle speed	DAS GPS	1 Hz
pedal_brake_state	Brake pedal state	Vehicle CAN	State change timestamps
pedal_gas_position	Gas pedal position	Vehicle CAN	Variable (1-100 Hz)

Table II: Metadata associated with each trip in the SHRP 2 dataset used in Surface Accelerations Reference.

Metadata type	Metadata description	Categories
Location	The state in which the vehicle was instrumented	New York Florida Washington North Carolina Pennsylvania Indiana
Age group	The age group of the participant	16-19 20-24 25-29 ⋮ 95-99
Gender	The gender of the participant	Male Female Did not specify
Vehicle class	The type of the vehicle used by the participant	Car Pickup SUV/Crossover Minivan

Table III: List of summary variables calculated for each acceleration epoch identified within a trip.

Summary Variable	Description
FILE_ID	Trip ID that uniquely identifies each trip in SHRP 2 dataset
TIME_START	Within trip start time of acceleration epoch
TIME_END	Within trip end time of acceleration epoch
ACCELERATION_X_MAX	Maximum acceleration value in epoch
ACCELERATION_X_MEAN	Mean acceleration value in epoch
ACCELERATION_X_MEDIAN	Median acceleration value in epoch
SPEED_START	Speed at start of epoch
SPEED_END	Speed at end of epoch
DISTANCE	Distance travelled in epoch
DURATION	Duration of epoch
SPEED_CHANGE	Difference in speed between end and start of epoch
ACCELERATION_SPEED_MEAN	Mean acceleration calculated from change in speed and duration
TIME_PEAK_ACCELERATION	Timestamp of peak acceleration during epoch
ACCELERATION_TO_PEAK_MEAN	Mean acceleration from start to peak of epoch
ACCELERATION_FROM_PEAK_MEAN	Mean acceleration from peak to end of epoch
SPEED_AT_PEAK_ACCEL	Speed at peak acceleration
SPEED_MAX	Maximum speed during the epoch
GAS_PEDAL_MEAN	Mean of gas pedal signal during the epoch
GAS_PEDAL_MEDIAN	Median of gas pedal signal during the epoch
GAS_PEDAL_MAX	Maximum of gas pedal signal during the epoch
GAS_PEDAL_MIN	Minimum of gas pedal signal during the epoch
GAS_PEDAL_STDEV	Standard deviation of gas pedal signal during the epoch
BRAKE	Whether brake was used during epoch
BRAKE_DURATION	Duration for which brake was used in epoch
FUNCTIONAL_CLASS	Functional class of the roadway at the time of peak acceleration
SPEED_CAT	Speed category of the roadway at the time of peak acceleration

## B. Creating Driver Acceleration Profiles from Summarized Epochs

Once all the acceleration epochs were identified, summarized, and recorded in the acceleration summary tables, a profile generation algorithm aggregated all epochs belonging to a driver-vehicle combination, creating a statistical profile. Such a profile was created for each of the following categories:

- Acceleration epochs
- Deceleration epochs
- Positive lateral acceleration epochs (vehicle moving towards right)
- Negative lateral acceleration epochs (vehicle moving towards left)

Three methods were used to compute statistical measures for each category to allow comparisons of various participants. Even though all three methods used the ACCELERATION\_X\_MAX (or equivalent measures for lateral acceleration), other measures mentioned in Table III, such as ACCELERATION\_X\_MEAN, could also be used. These methods are described in further detail in the following sections.

1) Comparing Percentiles: Using the percentile method, measures were computed at the 50<sup>th</sup>, 60<sup>th</sup>, 70<sup>th</sup>, 75<sup>th</sup>, 80<sup>th</sup>, 90<sup>th</sup>, 95<sup>th</sup>, 99<sup>th</sup>, and the 99.9<sup>th</sup> percentile. All epochs linked to a driver-vehicle combination were queried and the percentile values listed above were calculated for the maximum acceleration within the epoch. The percentiles allow users to compare frequent as well as rare epochs. For example, frequent epochs, such as 50<sup>th</sup> percentile (the stronger of two random epochs) to 90<sup>th</sup> percentile (the strongest of 10 random epochs), may indicate driving style, whereas rare epochs, such as 99<sup>th</sup> or 99.9<sup>th</sup> percentile, would indicate an atypical situation, either for the involved driver or nearby roadway users. This latter category may be indicative of potential safety critical events. In other words, the percentile measure relates the magnitude of the epoch and its rarity for each participant. Therefore, comparing drivers on the same percentile shows the difference in magnitude for equally rare epochs. An example finding would be that for one driver or group of drivers, an 80<sup>th</sup> percentile epoch would be 0.2 g deceleration whereas for another driver or group of drivers, the 80<sup>th</sup> percentile epoch would be 0.3 g deceleration. The latter driver/group of drivers would execute hard decelerations much more often, though this metric cannot reveal how often per mile the behavior occurred.

2) Comparing Rate of Epochs Stronger Than a Threshold Magnitude: This method measured the rate of epochs stronger than a certain threshold per mile. The following rates were calculated:

- Number of epochs stronger than 0.1g per mile/kilometer

- Number of epochs stronger than 0.2g per mile/kilometer
- Number of epochs stronger than 0.3g per mile/kilometer
- Number of epochs stronger than 0.4g per mile/kilometer
- Number of epochs stronger than 0.5g per mile/kilometer
- Number of epochs stronger than 0.6g per mile/kilometer
- Number of epochs stronger than 0.7g per mile/kilometer
- Number of epochs stronger than 0.8g per mile/kilometer
- Number of epochs stronger than 0.9g per mile/kilometer

These metrics were calculated using Equation 1

$$R_X = \frac{N_X}{D_T} \quad (1)$$

where  $R_x$  is the rate of epochs stronger than  $X$ (g) per mile,  $N_X$  is the number of epochs stronger than  $X$ (g), and  $D_T$  is the total distance traveled by the participant. The different thresholds used to calculate these metrics differentiate epochs based on their severity. This measure compares the frequency of epochs stronger than a particular threshold among various drivers. The rates for different thresholds can have different implications. For example, for lower thresholds, the rates would imply a higher number of epochs per mile that can be caused by numerous factors, such as traffic, road type, and driving style. Higher thresholds could imply a stronger correlation to safety critical events. Through this metric it is possible to understand the range of amplitudes and frequency of acceleration epochs per unit distance traveled.

3) Comparing the Strongest Epoch in a Threshold Distance: This method compared participants based on the strongest epoch they experienced within a certain driving distance. The following measures were calculated using this method:

- Strongest epoch experienced in 1 mile/kilometer
- Strongest epoch experienced in 5 miles/kilometers
- Strongest epoch experienced in 10 miles/kilometers
- Strongest epoch experienced in 50 miles/kilometers
- Strongest epoch experienced in 100 miles/kilometers
- Strongest epoch experienced in 1000 miles/kilometers.

To calculate the strongest epoch experienced in a certain distance, the percentile equivalent of that distance was first calculated. Equation 2,

$$\lambda_z = \frac{\left(1 - \frac{z}{100}\right) \times N_T}{D_T} \quad (2)$$

shows the rate of epochs,  $\lambda_Z$ , above the  $Z^{th}$  percentile, with  $N_T$  being the total number of epochs experienced and  $D_T$  being the total distance travelled. The distance travelled per  $Z^{th}$  percentile epoch is therefore given by inverting the equation as follows in Equation 3:

$$\zeta = \frac{1}{\lambda_Z} = \frac{D_T}{\left(1 - \frac{Z}{100}\right) \times N_T} \quad (3)$$

Therefore, on average, the  $Z^{th}$  percentile epoch is the strongest epoch in  $\zeta$  miles. To calculate the strongest epoch in a certain distance, say  $\zeta = Y$  miles, the corresponding percentile can be found using Equation 4:

$$Z = 100 \times \left(1 - \frac{D_T}{Y \times N_T}\right) \quad (4)$$

Since the epoch rate,  $N_T/D_T$ , is different for different drivers, equation 4 allows a comparison of drivers based on unequal percentiles that correspond to an equal amount of driving.

Like the other statistical measures used to create the profile, these measures also allow driver comparison for frequent (strongest epoch experienced in 1 mile) as well as rare epochs (strongest epoch in 100 miles). This approach enables users of the Surface Acceleration Reference to identify what extreme epoch might be expected within a certain distance of travel, and is important for understanding the differences in epochs that are due to driving style versus those that are due to adverse events. The three categories of measures together provide a comprehensive driving profile for each participant in the SHRP 2 dataset and return units of analysis that are useful for users from multiple domains. All three types of measures were contextualized by roadway functional class and speed category on which they occurred. These measures have been made available for download in the form of a CSV file here.

### C. Creating Interactive Visualization from Driver Acceleration Profiles

To achieve the project's purpose of creating an easily accessible dataset for a wide variety of users from various fields and backgrounds, it was important to have a low-effort threshold for data analysis. Even though the statistical driving profile for each participant is available via a downloadable CSV file, considerable effort is still required to ingest the data, understand its structure, and make meaningful inferences. To lower this threshold, a web app based on the same dataset was developed using R, ggplot2, and Shiny [48]–[50]. This web app can be accessed through any web browser at [dataviz.vtti.vt.edu/Surface\\_Accelerations\\_Reference/](http://dataviz.vtti.vt.edu/Surface_Accelerations_Reference/). This interface allows researchers to compare SHRP 2 participants on any and all of the aforementioned measures with the ability to interrogate data by age,

gender, location, and vehicle type. Figure 4 shows an example comparison for rate of epochs greater than 0.3 g where the data has been parsed by gender (category shown on right side of charts) along the vertical axis and age along the horizontal axis (category shown on top of charts).

Figure 4 provides an example of one combination of conditions that can be created using the visualization tool. Across all plots that might be created using the visualization tool, each mark in a plot represents one participant. The mark's position along the y-axis represents the measures described previously (i.e., percentile value, epoch rate, etc.) for a specific driver. The position of a point along the x-axis is randomly generated noise that aids visualization by reducing overlapping points. As illustrated in the legend in Figure 5, across plots, the size of a mark represents the amount of driving in the study and the shape and color represent the vehicle class. The various plot tiles or cells represent the categories to which each driver belongs making it easy to compare different classes. A box plot is overlaid on the scatter plot to show the median, quantiles and the outliers of the distribution. Hovering over a data point reveals additional information about the driver, including the exact value of the measure, gender, age, vehicle class, and total distance in the study. In addition, users are provided the ability to choose the units of distance, clip outliers for better resolution, display summary statistics, and plot the kernel distribution of the group in the form of a violin plot.

## III. Findings

The main purpose of this project was to create an accessible catalog of accelerations experienced by road users in passenger vehicles that would enable users to answer questions pertinent to their fields. Therefore, most of the findings will come from the exploration of the Surface Accelerations Reference dataset and visualization tool. As an example of its application, differences in rates of accelerations on roads of various road speed categories are explored below.

Figure 5 shows the variation of epoch rates at the various maximum deceleration thresholds for all participants in SHRP 2 NDS grouped by the road speed category. The box plots show the distribution of rates at key thresholds and the dashed line represents the median calculated at a finer resolution. The threshold magnitudes are scaled linearly and the epoch rates are scaled logarithmically. A zero value for the median or the 25<sup>th</sup> percentile lies at  $-\infty$  on a log scale and therefore, is shown by keeping the box plot open. Figures 6, 7, and 8 describe similar information for longitudinal accelerations, lateral neagitive accelerations (left leaning), and lateral positive accelerations (right leaning) respectively.

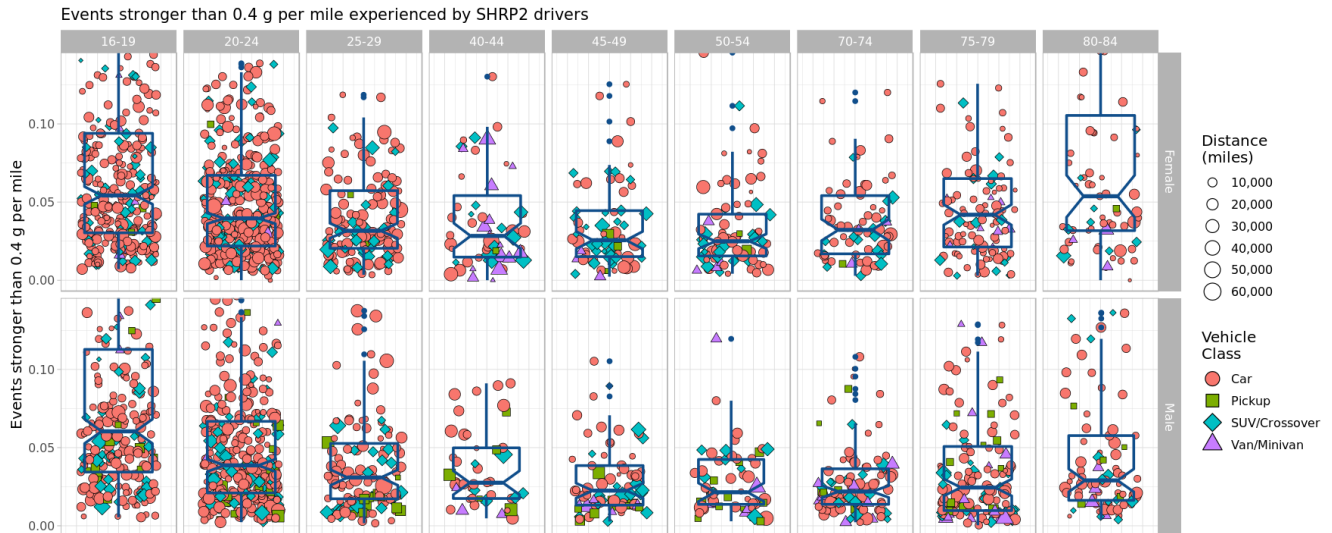


Figure 4: Interactive visualization available via the Surface Acceleration Reference web app comparing data based on age range and gender.

The relationship between the epoch rates and the deceleration thresholds is log piecewise linear, i.e., the rate decreases exponentially as the threshold is increased linearly. Within the epoch rate distribution at each threshold, the rates for individual road speed categories differ by 1 to 2 orders of magnitude. For example, the deceleration epoch rate for the maximum deceleration threshold of 0.2 g is 2.8 epochs per mile for < 31 mph roads and 2.8 epoch per 100 miles for 65-80 mph roads. Tables IV, V, VII, and VI in the Appendix list the values of the 25<sup>th</sup>, 50<sup>th</sup>, and 75<sup>th</sup> percentile epoch rates at key maximum acceleration thresholds.

Within each distribution shown in Figures 5, 6, 7, and 8 the interquartile range is significant and increases with road speed as well as g-force magnitude. This implies that kinematic behaviour of the various participants has a higher variance for stronger thresholds. In other words, the proportional difference in rate between participants increases for stronger threshold epoch as well as on higher speed roads. These differences between various drivers can be explored using the accelerations reference and valuable insights can be drawn about driver kinematic behaviour.

These inferences will be useful across a number of fields. For example, designers of advanced driver assistance and automated driving systems can use Figures 5 to 8 and Tables IV to VII to compare the accelerations produced by their systems to a diverse driving population while controlling for roadway speed. This will enable system tuning to match certain driving populations such as the median driver or a driver in the interquartile range.

Organizations analyzing cohort data such as ride share

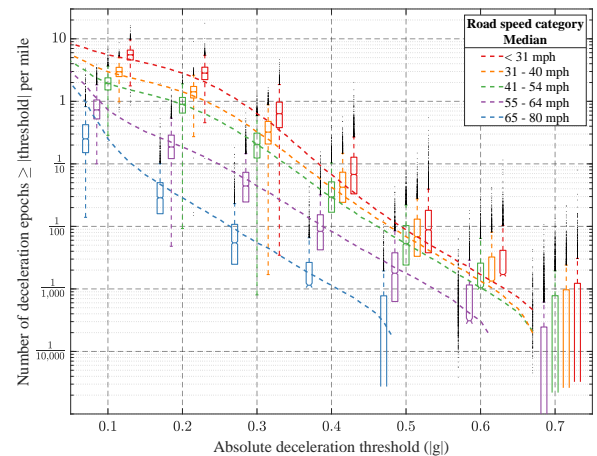


Figure 5: Comparison of driver epoch rates at various maximum deceleration thresholds.

service providers and taxi companies will be able to use the Surface Accelerations Reference for comparisons of their drivers with a national driving population. Similarly, “pay as you drive” and “pay how you drive” insurance programs will be able to utilize this data to compare their customers with a standardized national distribution allowing more transparency and, therefore, better adoption.

#### IV. Conclusions

This study fulfills three major unmet needs in the study of accelerations based driving characteristics. First, the Surface Acceleration Reference provides a representative catalog of lateral and longitudinal accelerations in the form of a downloadable dataset and interactive analytics tool available at

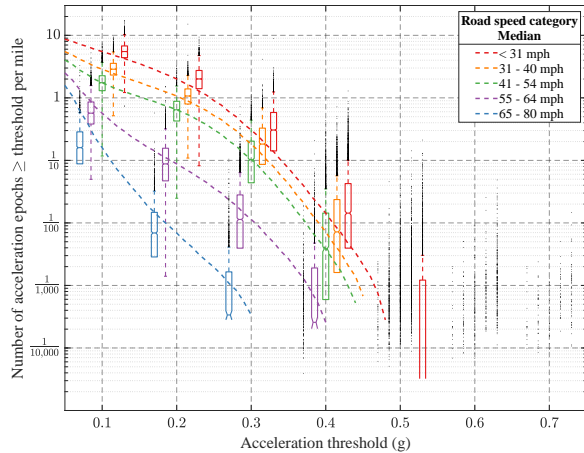


Figure 6: Comparison of driver epoch rates at various maximum acceleration thresholds.

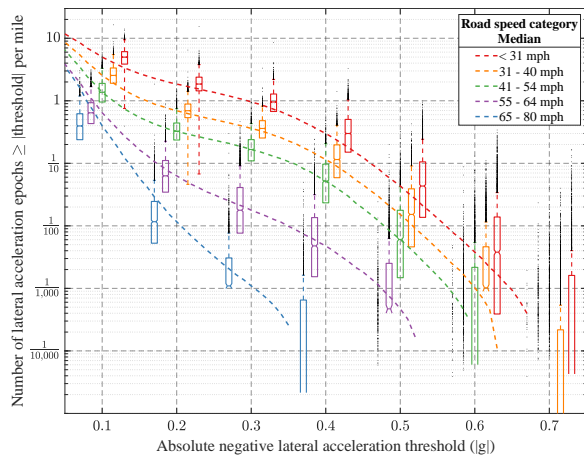


Figure 7: Comparison of driver epoch rates at various maximum negative lateral acceleration (left leaning) thresholds.

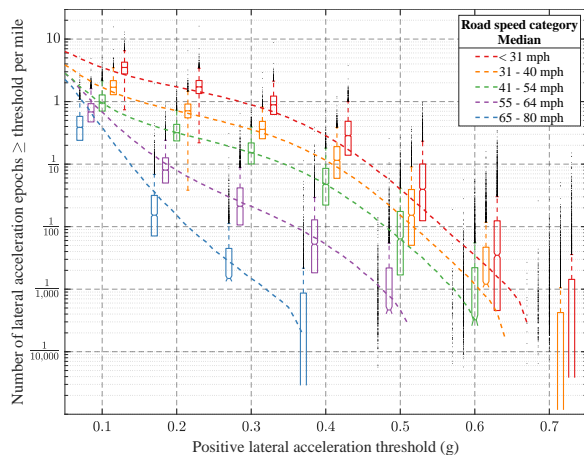


Figure 8: Comparison of driver epoch rates at various maximum positive lateral acceleration (right leaning) thresholds.

[dataviz.vtti.vt.edu/Surface\\_Accelerations\\_Reference/](http://dataviz.vtti.vt.edu/Surface_Accelerations_Reference/). This catalog summarizes the acceleration behavior of over 3,500 participants in the SHRP2 NDS and is the largest openly available dataset of its kind. It can benefit a number of fields. For example, it will facilitate intelligent vehicle system engineers to design systems that safer and better representative of driver preferences. It will also enable behavioral researchers to understand the effect of various roadway, driver, and vehicle characteristics on the frequency and magnitude of accelerations.

Second, this paper introduces a methodology to create a standardized catalog of accelerations that can be replicated on similar datasets. A standardized approach has been missing in the field of acceleration behavior as different studies have used varying methods of comparing accelerations across populations. An algorithm was developed to summarize all the acceleration epochs in a driver's history to create profiles describing each participants acceleration norms and frequencies at different levels. This methodology includes signal processing, epoch definitions, summary extraction and standardization techniques. The statistical profiles created for every driver had three types of measures based on percentiles, rates, and distance thresholds, which makes this methodology applicable for a wide array of fields. This methodology can be used by agencies having similar datasets such as vehicle fleet operators, ride share services, government departments of transportation, and research institutes around the world to compare driving populations.

Finally, an analysis was conducted to measure the effect of road speed category on the distribution of longitudinal and lateral acceleration rates. It was observed that lower speed roads (< 31 mph) have 2 to 3 orders of magnitude higher rates of strong g-force events as compared to high speed roads (65-80 mph). It was also observed that the relationship between the rate of epochs (i.e., accelerations) and the g-force magnitude was log-piecewise linear. I.e., for a linear increase in g-force magnitude, the rate of occurrence decreases exponentially. Even when controlling for the road speed category, the variance for high g-force events was significant and could indicate differences in driving style and effects of traffic conditions, driver demographics, etc.

Intelligent driving systems such as ADAS and automated vehicles interact with drivers, passengers, and other road users in safety critical ways with very little margin for error. Therefore, it is essential that such systems are developed based on data accurately representing the breadth of human behaviors and driving environments. The Surface Accelerations Reference provides a large-scale, real-world, diverse, and context rich catalog of accelerations. In addition to vehicle system development, these data will also provide value to many transportation

related fields such as roadway, vehicle and safety systems design.

#### Acknowledgements

This work was supported by The National Surface Transportation Safety Center for Excellence (NSTSC) at Virginia Tech Transportation Institute (VTTI).

#### Supplementary data

The acceleration profiles described in this paper are available for download at: <https://github.com/gibranal/surface-accelerations-reference>.

#### References

- [1] T. A. Dingus, J. M. Hankey, J. F. Antin, S. E. Lee, L. Eichelberger, K. Stulce, D. McGraw, M. a. S. P. Loren, Strategic Highway Research Program Safety Focus Area, Transportation Research Board, and National Academies of Sciences, Engineering, and Medicine, Naturalistic driving study: Technical coordination and quality control. Washington, D.C.: Transportation Research Board, Mar. 22, 2014.
- [2] S. Le Vine, A. Zolfaghari, and J. Polak, "Autonomous cars: The tension between occupant experience and intersection capacity," *Transportation Research Part C: Emerging Technologies*, vol. 52, pp. 1–14, Mar. 2015.
- [3] R. M. Brooks, "Acceleration characteristics of vehicles in rural pennsylvania," 2012.
- [4] G. Ali, S. McLaughlin, and M. Ahmadian, "Quantifying the effect of roadway, driver, vehicle, and location characteristics on the frequency of longitudinal and lateral accelerations," *Accident Analysis & Prevention*, vol. 161, p. 106 356, Oct. 1, 2021.
- [5] J. M. Scanlon, R. Sherony, and H. C. Gabler, "Models of driver acceleration behavior prior to real-world intersection crashes," *IEEE Transactions on Intelligent Transportation Systems*, vol. 19, no. 3, pp. 774–786, Mar. 2018.
- [6] G. Li, F. Zhu, X. Qu, B. Cheng, S. Li, and P. Green, "Driving style classification based on driving operational pictures," *IEEE Access*, vol. 7, pp. 90 180–90 189, 2019.
- [7] V. Vaitkus, P. Lengvenis, and G. Žylius, "Driving style classification using long-term accelerometer information," in *2014 19th international conference on methods and models in automation and robotics (MMAR)*, Sep. 2014, pp. 641–644.
- [8] M. V. Ly, S. Martin, and M. M. Trivedi, "Driver classification and driving style recognition using inertial sensors," in *2013 IEEE intelligent vehicles symposium (IV)*, Jun. 2013, pp. 1040–1045.
- [9] C. Sohn, J. Andert, and R. N. N. Manfou, "A driveability study on automated longitudinal vehicle control," *IEEE Transactions on Intelligent Transportation Systems*, vol. 21, no. 8, pp. 3273–3280, Aug. 2020.
- [10] V. A. Butakov and P. A. Ioannou, "Driver/vehicle response diagnostic system for the vehicle-following case," *IEEE Transactions on Intelligent Transportation Systems*, vol. 15, no. 5, pp. 1947–1957, Oct. 2014.
- [11] B. Higgs and M. Abbas, "Segmentation and clustering of car-following behavior: Recognition of driving patterns," *IEEE Transactions on Intelligent Transportation Systems*, vol. 16, no. 1, pp. 81–90, Feb. 2015.
- [12] S. G. Christopoulos, S. Kanarachos, and A. Chronos, "Learning driver braking behavior using smartphones, neural networks and the sliding correlation coefficient: Road anomaly case study," *IEEE Transactions on Intelligent Transportation Systems*, vol. 20, no. 1, pp. 65–74, Jan. 2019.
- [13] B. Ciuffo, M. Makridis, T. Toledo, and G. Fontaras, "Capability of current car-following models to reproduce vehicle free-flow acceleration dynamics," *IEEE Transactions on Intelligent Transportation Systems*, vol. 19, no. 11, pp. 3594–3603, Nov. 2018.
- [14] H. A. Rakha, K. Ahn, W. Faris, and K. S. Moran, "Simple vehicle powertrain model for modeling intelligent vehicle applications," *IEEE Transactions on Intelligent Transportation Systems*, vol. 13, no. 2, pp. 770–780, Jun. 2012.
- [15] V. A. Butakov and P. Ioannou, "Personalized driver assistance for signalized intersections using v2i communication," *IEEE Transactions on Intelligent Transportation Systems*, vol. 17, no. 7, pp. 1910–1919, Jul. 2016.
- [16] C. Miyajima, H. Ukai, A. Naito, H. Amata, N. Kitaoka, and K. Takeda, "Driver risk evaluation based on acceleration, deceleration, and steering behavior," in *2011 IEEE international conference on acoustics, speech and signal processing (ICASSP)*, May 2011, pp. 1829–1832.
- [17] A. B. R. González, M. R. Wilby, J. J. V. Díaz, and C. S. Ávila, "Modeling and detecting aggressiveness from driving signals," *IEEE Transactions on Intelligent Transportation Systems*, vol. 15, no. 4, pp. 1419–1428, Aug. 2014.
- [18] B. Zhu, Y. Jiang, J. Zhao, R. He, N. Bian, and W. Deng, "Typical-driving-style-oriented personalized adaptive cruise control design based on human driving data," *Transportation Research Part C: Emerging Technologies*, vol. 100, pp. 274–288, Mar. 1, 2019.
- [19] Policy on geometric design of highways and streets (5th edition). Place of publication not identified:

- American Association of State Highway and Transportation Officials (AASHTO), 2004.
- [20] D. B. Fambro, K. Fitzpatrick, and R. J. Koppa, Determination of stopping sight distances. Transportation Research Board, 1997.
- [21] G. Long, "Acceleration characteristics of starting vehicles," Transportation Research Record: Journal of the Transportation Research Board, vol. 1737, no. 1, pp. 58–70, Jan. 2000.
- [22] D. V. McGehee, M. Raby, C. Carney, J. D. Lee, and M. L. Reyes, "Extending parental mentoring using an event-triggered video intervention in rural teen drivers," Journal of Safety Research, vol. 38, no. 2, pp. 215–227, Jan. 2007.
- [23] O. Musicant and L. Lampel, "When technology tells novice drivers how to drive," Transportation Research Record: Journal of the Transportation Research Board, vol. 2182, no. 1, pp. 8–15, Jan. 2010.
- [24] L. Eboli, G. Mazzulla, and G. Pungillo, "Combining speed and acceleration to define car users' safe or unsafe driving behaviour," Transportation Research Part C: Emerging Technologies, vol. 68, pp. 113–125, Jul. 1, 2016.
- [25] M. R. Carlos, L. C. González, J. Wahlström, G. Ramírez, F. Martínez, and G. Runger, "How smartphone accelerometers reveal aggressive driving behavior?—the key is the representation," IEEE Transactions on Intelligent Transportation Systems, vol. 21, no. 8, pp. 3377–3387, Aug. 2020.
- [26] G. Castignani, T. Derrmann, R. Frank, and T. Engel, "Driver behavior profiling using smartphones: A low-cost platform for driver monitoring," IEEE Intelligent Transportation Systems Magazine, vol. 7, no. 1, pp. 91–102, 2015.
- [27] B. G. Simons-Morton, Z. Zhang, J. C. Jackson, and P. S. Albert, "Do elevated gravitational-force events while driving predict crashes and near crashes?" American Journal of Epidemiology, vol. 175, no. 10, pp. 1075–1079, May 15, 2012.
- [28] O. Musicant, H. Bar-Gera, and E. Schechtman, "Temporal perspective on individual driver behavior using electronic records of undesirable events," Accident Analysis & Prevention, vol. 70, pp. 55–64, Sep. 2014.
- [29] Yilin Zhao, "Telematics: Safe and fun driving," IEEE Intelligent Systems, vol. 17, no. 1, pp. 10–14, Jan. 2002.
- [30] T. Litman, "Pay-as-you-drive pricing and insurance regulatory objectives.," Journal of Insurance Regulation, vol. 23, no. 3, 2005.
- [31] P. Handel, I. Skog, J. Wahlstrom, F. Bonawiede, R. Welch, J. Ohlsson, and M. Ohlsson, "Insurance telematics: Opportunities and challenges with the smartphone solution," IEEE Intelligent Transportation Systems Magazine, vol. 6, no. 4, pp. 57–70, 2014.
- [32] D. I. Tselentis, G. Yannis, and E. I. Vlahogianni, "Innovative motor insurance schemes: A review of current practices and emerging challenges," Accident Analysis & Prevention, vol. 98, pp. 139–148, Jan. 1, 2017.
- [33] R. Akçelik and M. Besley, "Acceleration and deceleration models," in 23rd conference of Australian institutes of transport research (CAITR 2001), Monash University, Melbourne, Australia, Dec. 10, 2001, pp. 10–12.
- [34] J. Wang, K. K. Dixon, H. Li, and J. Ogle, "Normal acceleration behavior of passenger vehicles starting from rest at all-way stop-controlled intersections," Transportation Research Record: Journal of the Transportation Research Board, vol. 1883, no. 1, pp. 158–166, Jan. 2004.
- [35] T. Toledo, H. N. Koutsopoulos, and M. Ben-Akiva, "Integrated driving behavior modeling," Transportation Research Part C: Emerging Technologies, vol. 15, no. 2, pp. 96–112, Apr. 1, 2007.
- [36] J. F. Torres, "Acceleration noise, power spectra, and other statistics derived from instrumented vehicle measurements under freeway driving conditions," Highway Research Record, no. 308, 1970.
- [37] L. L. Hoberock, "A survey of longitudinal acceleration comfort studies in ground transportation vehicles," Journal of Dynamic Systems, Measurement, and Control, vol. 99, no. 2, p. 76, 1977.
- [38] D. Litwhiler and D. Martin, "An investigation of acceleration and jerk profiles of public transportation vehicles," p. 13,
- [39] C. Abernethy, G. Plank, E. D. Sussman, and H. Jacobs, Effects of deceleration and rate of deceleration on live seated human subjects. Urban Mass Transportation Administration, 1977.
- [40] C. C. Smith, D. Y. McGehee, and A. J. Healey, "The prediction of passenger riding comfort from acceleration data," Journal of Dynamic Systems, Measurement, and Control, vol. 100, no. 1, p. 34, 1978.
- [41] J. B. Ferris, "Factors affecting perceptions of ride quality in automobiles," vol. 65, p. 6, 1999.
- [42] J. Antin, K. Stulce, L. Eichelberger, J. Hankey, Strategic Highway Research Program Safety Focus Area, Transportation Research Board, and National Academies of Sciences, Engineering, and Medicine, Naturalistic driving study: descriptive comparison of the study sample with national data. Washington, D.C.: Transportation Research Board, Feb. 28, 2015.
- [43] STMicroelectronics. (Oct. 2005). LIS3lv02dq MEMS inertial sensor, [Online]. Available: <https://www.mouser.com/datasheet/2/389/>

stmicroelectronics\_cd00047926-330956.pdf (visited on 10/12/2022).

- [44] T. Müller, H. Hajek, L. Radić-Weißefeld, and K. Bengler, “Can you feel the difference? the just noticeable difference of longitudinal acceleration,” Proceedings of the Human Factors and Ergonomics Society Annual Meeting, vol. 57, no. 1, pp. 1219–1223, Sep. 2013.
- [45] S. B. McLaughlin and J. M. Hankey, “Matching GPS records to digital map data: Algorithm overview and application,” National Surface Transportation Safety Center for Excellence, 15-UT-033, Mar. 3, 2015.
- [46] Here Technologies. (Mar. 2, 2019). FunctionalClassType - routing API - HERE developer, FunctionalClassType - routing API - HERE Developer, [Online]. Available: <https://developer.here.com/documentation/routing/topics/resource-type-functional-class.html> (visited on 03/02/2019).
- [47] Here Technologies. (Mar. 2, 2019). SpeedCategoryType - geocoder API - HERE developer, SpeedCategoryType - geocoder API - HERE Developer, [Online]. Available: <https://developer.here.com/documentation/geocoder/topics/resource-type-speed-category.html> (visited on 03/02/2019).
- [48] W. Chang, J. Cheng, J. J. Allaire, Y. Xie, and J. McPherson, “Shiny: Web application framework for r,” R package version 0.11, vol. 1, no. 4, p. 106, 2015.
- [49] H. Wickham, ggplot2: Elegant graphics for data analysis, ser. Use r! New York: Springer-Verlag, 2009.
- [50] H. Wickham, R. Francois, L. Henry, and K Müller, “Dplyr: A grammar of data manipulation,” R package version 0.4, vol. 3, 2015.



Gibran Ali is a vehicle systems and data engineer working in the Division of Data and Analytics at Virginia Tech Transportation Institute (VTTI) since 2016. He received his B.Tech. in mechanical engineering from National Institute of Technology Srinagar in 2010, his M.S. in mechanical engineering from Clemson University in 2014 and Ph.D. in mechanical engineering from Virginia Tech in 2022. Previously, he has worked at the R&D center of Mahindra Automobiles

from 2010 to 2012 as a drivetrain simulation and performance engineer. His previous research work include energy harvesting, control systems, and mechatronics.

Gibran’s current research involves analyzing large scale datasets such as the SHRP2-NDS using various data processing, analytics, machine learning, and mathematical modeling techniques. These analyses are conducted to improve vehicle system design and further the understanding of driver behavior. He specializes in creating data based interactive analytics tools that integrate human, vehicle system, and environmental factors to further roadway safety.



Shane McLaughlin has been active conducting driving related data collection and large-scale analysis projects supporting industry and the public sector for over 20 years. Throughout, his emphasis has been work that involves vehicle control systems, characterization of the driving context, and the behavior and performance capabilities of humans. In 2022, he formed Great Iris LLC, through which he assists clients as they engineer, test, and deploy increasingly

capable sensing, planning, and control systems.

Shane holds a B.S. in Engineering Science and Mechanics from Virginia Tech, where he also completed his M.S. and Ph.D. Shane started his career at Ford Motor Company in Systems Safety and Human Factors and Ergonomics. After Ford he worked in a variety of roles at the Virginia Tech Transportation Institute. In 2017 Shane was nominated by the U.S. Secretary of Transportation to the Federal Motorcyclist Advisory Council based on nationally recognized expertise in both automated-vehicle systems and motorcycle rider safety.



Mehdi Ahmadian is J. Bernard Jones Chair in Mechanical Engineering at Virginia Tech, where he also holds the position of Director of Center for Vehicle Systems and Safety (CVeSS), and the Railway Technologies Laboratory (RTL). Prior to joining Virginia Tech in 1995, Mehdi worked in the transportation industry for eight years, including serving as the Lead Design Engineer for steerable locomotive trucks (bogies) at General Electric Transportation System from 1993 – 1995. He has authored four book chapters, more than 150 archival journal papers, and more than 400 conference publications and presentations, including numerous major keynote and plenary lectures, and invited presentations. He holds 11 U.S. and international patents.

Mehdi is a Fellow of the American Society of Mechanical Engineers (ASME), Fellow of the Society of Automotive Engineers (SAE International), and Associate Fellow of the American Institute for Aeronautics and Astronautics (AIAA). His most recent professional awards include the 2019 Magnus Hendrickson Innovation Award, the 2015 SAE Lloyd L. Withrow Distinguished Speaker Award; and the 2014 SAE International L. Ray Buckendale Award with a plenary lecture on “Integrating Electromechanical Systems in Commercial Vehicles for Improved Handling, Stability, and Comfort.”

## Appendix Supplementary Tables

Table IV: The 25<sup>th</sup>, 50<sup>th</sup>, and 75<sup>th</sup> percentile deceleration epoch rates for all drivers at various thresholds grouped by road speed category.

Road speed category (mph)	Measure (%tiles)	Rate of epochs per mile greater than threshold					
		0.1 (g)	0.2 (g)	0.3 (g)	0.4 (g)	0.5 (g)	0.6 (g)
All	25	2.2E+00	9.3E-01	1.7E-01	1.9E-02	2.7E-03	4.7E-04
All	50	2.9E+00	1.3E+00	2.8E-01	3.4E-02	5.3E-03	1.1E-03
All	75	3.7E+00	1.8E+00	4.6E-01	6.5E-02	1.0E-02	2.4E-03
<31	25	4.6E+00	2.2E+00	3.8E-01	3.3E-02	3.8E-03	0
<31	50	5.5E+00	2.8E+00	6.3E-01	6.7E-02	8.8E-03	1.7E-03
<31	75	6.6E+00	3.5E+00	9.7E-01	1.3E-01	1.8E-02	4.1E-03
31 - 40	25	2.5E+00	1.1E+00	2.1E-01	2.4E-02	3.3E-03	0
31 - 40	50	3.0E+00	1.4E+00	3.2E-01	4.2E-02	6.8E-03	1.3E-03
31 - 40	75	3.5E+00	1.7E+00	4.7E-01	7.3E-02	1.3E-02	3.2E-03
41 - 54	25	1.5E+00	6.3E-01	1.2E-01	1.6E-02	2.3E-03	0
41 - 54	50	1.9E+00	8.8E-01	2.0E-01	2.9E-02	5.3E-03	9.7E-04
41 - 54	75	2.4E+00	1.1E+00	3.1E-01	5.1E-02	1.0E-02	2.6E-03
55 - 64	25	5.2E-01	1.2E-01	2.5E-02	4.2E-03	5.2E-04	0
55 - 64	50	7.3E-01	1.9E-01	4.5E-02	8.3E-03	1.7E-03	2.1E-04
55 - 64	75	1.0E+00	2.9E-01	7.4E-02	1.5E-02	3.8E-03	1.1E-03
65 - 80	25	1.5E-01	1.5E-02	2.3E-03	0	0	0
65 - 80	50	2.5E-01	2.8E-02	5.2E-03	1.0E-03	0	0
65 - 80	75	4.1E-01	4.9E-02	1.1E-02	2.6E-03	6.8E-04	0

Table V: The 25<sup>th</sup>, 50<sup>th</sup>, and 75<sup>th</sup> percentile acceleration epoch rates for all drivers at various thresholds grouped by road speed category.

Road speed category (mph)	Measure (%tiles)	Rate of epochs per mile greater than threshold					
		0.1 (g)	0.2 (g)	0.3 (g)	0.4 (g)	0.5 (g)	0.6 (g)
All	25	1.9E+00	6.0E-01	6.7E-02	2.0E-03	0	0
All	50	2.6E+00	8.8E-01	1.4E-01	6.8E-03	1.0E-04	0
All	75	3.5E+00	1.3E+00	2.7E-01	2.1E-02	5.6E-04	0
<30 mph	25	4.4E+00	1.4E+00	1.4E-01	4.0E-03	0	0
<30 mph	50	5.5E+00	2.0E+00	3.1E-01	1.4E-02	0	0
<30 mph	75	6.8E+00	2.7E+00	5.9E-01	4.3E-02	1.2E-03	0
31 - 40	25	2.3E+00	7.9E-01	8.5E-02	1.6E-03	0	0
31 - 40	50	2.9E+00	1.1E+00	1.8E-01	7.3E-03	0	0
31 - 40	75	3.6E+00	1.4E+00	3.3E-01	2.4E-02	0	0
41 - 54	25	1.3E+00	4.1E-01	4.1E-02	4.3E-04	0	0
41 - 54	50	1.7E+00	6.3E-01	1.0E-01	3.7E-03	0	0
41 - 54	75	2.2E+00	8.7E-01	2.0E-01	1.4E-02	0	0
55- 64	25	3.8E-01	4.7E-02	3.9E-03	0	0	0
55- 64	50	5.7E-01	9.0E-02	1.2E-02	1.6E-04	0	0
55- 64	75	8.6E-01	1.6E-01	2.9E-02	1.9E-03	0	0
65 - 80	25	8.7E-02	2.6E-03	0	0	0	0
65 - 80	50	1.6E-01	6.6E-03	1.2E-04	0	0	0
65 - 80	75	2.8E-01	1.5E-02	1.6E-03	0	0	0

Table VI: The 25<sup>th</sup>, 50<sup>th</sup>, and 75<sup>th</sup> percentile lateral positive acceleration epoch rates for all drivers at various thresholds grouped by road speed category.

Road speed category (mph)	Measure (%tiles)	Rate of epochs per mile greater than threshold					
		0.1 (g)	0.2 (g)	0.3 (g)	0.4 (g)	0.5 (g)	0.6 (g)
All	25	1.4E+00	5.7E-01	2.5E-01	5.8E-02	6.4E-03	4.7E-04
All	50	1.8E+00	7.7E-01	3.7E-01	1.2E-01	1.8E-02	2.0E-03
All	75	2.3E+00	1.0E+00	5.2E-01	2.0E-01	4.2E-02	6.2E-03
<30 mph	25	2.7E+00	1.3E+00	6.2E-01	1.4E-01	1.2E-02	4.0E-04
<30 mph	50	3.5E+00	1.7E+00	8.9E-01	2.9E-01	4.0E-02	3.5E-03
<30 mph	75	4.3E+00	2.2E+00	1.2E+00	4.9E-01	1.0E-01	1.2E-02
31 - 40	25	1.3E+00	5.5E-01	2.5E-01	5.8E-02	4.9E-03	0
31 - 40	50	1.7E+00	7.1E-01	3.6E-01	1.1E-01	1.5E-02	1.1E-03
31 - 40	75	2.1E+00	9.1E-01	4.8E-01	1.9E-01	3.9E-02	4.7E-03
41 - 54	25	6.9E-01	2.3E-01	9.7E-02	2.1E-02	1.5E-03	0
41 - 54	50	9.4E-01	3.2E-01	1.5E-01	4.6E-02	6.2E-03	1.9E-04
41 - 54	75	1.3E+00	4.3E-01	2.2E-01	8.4E-02	1.7E-02	2.2E-03
55- 64	25	4.5E-01	4.8E-02	1.1E-02	1.7E-03	0	0
55- 64	50	6.7E-01	7.9E-02	2.1E-02	5.3E-03	4.0E-04	0
55- 64	75	9.2E-01	1.3E-01	4.2E-02	1.3E-02	2.2E-03	0
65 - 80	25	2.4E-01	6.7E-03	0	0	0	0
65 - 80	50	3.8E-01	1.5E-02	1.3E-03	0	0	0
65 - 80	75	5.8E-01	3.2E-02	4.4E-03	7.6E-04	0	0

Table VII: The 25<sup>th</sup>, 50<sup>th</sup>, and 75<sup>th</sup> percentile lateral negative acceleration epoch rates for all drivers at various thresholds grouped by road speed category.

Road speed category (mph)	Measure (%tiles)	Rate of epochs per mile greater than threshold					
		0.1 (g)	0.2 (g)	0.3 (g)	0.4 (g)	0.5 (g)	0.6 (g)
All	25	1.8E+00	5.8E-01	2.6E-01	6.1E-02	6.0E-03	4.3E-04
All	50	2.4E+00	7.9E-01	3.8E-01	1.2E-01	1.8E-02	1.7E-03
All	75	3.2E+00	1.1E+00	5.5E-01	2.0E-01	4.2E-02	5.9E-03
<30 mph	25	3.9E+00	1.4E+00	6.8E-01	1.5E-01	1.4E-02	4.5E-04
<30 mph	50	5.0E+00	1.9E+00	9.6E-01	3.0E-01	4.4E-02	3.8E-03
<30 mph	75	6.1E+00	2.4E+00	1.3E+00	5.1E-01	1.1E-01	1.4E-02
31 - 40	25	1.9E+00	5.3E-01	2.5E-01	5.9E-02	4.6E-03	0
31 - 40	50	2.5E+00	6.9E-01	3.6E-01	1.2E-01	1.5E-02	1.0E-03
31 - 40	75	3.3E+00	8.9E-01	4.8E-01	2.0E-01	3.9E-02	4.6E-03
41 - 54	25	9.4E-01	2.3E-01	1.1E-01	2.3E-02	1.4E-03	0
41 - 54	50	1.3E+00	3.2E-01	1.6E-01	5.1E-02	6.1E-03	0
41 - 54	75	1.9E+00	4.4E-01	2.4E-01	9.7E-02	1.8E-02	2.1E-03
55- 64	25	4.2E-01	3.4E-02	7.4E-03	1.4E-03	0	0
55- 64	50	6.4E-01	6.2E-02	1.8E-02	4.7E-03	4.1E-04	0
55- 64	75	9.2E-01	1.1E-01	4.1E-02	1.3E-02	2.5E-03	0
65 - 80	25	2.3E-01	5.1E-03	0	0	0	0
65 - 80	50	3.9E-01	1.1E-02	9.9E-04	0	0	0
65 - 80	75	6.2E-01	2.5E-02	3.1E-03	6.0E-04	0	0